Phosphate starvation response precedes drought response in field-grown plants

Yukari Nagatoshi[1], Kenta Ikazaki[2], Nobuyuki Mizuno[3†], Yasufumi Kobayashi[1], Kenichiro Fujii[1], Eri Ogiso-Tanaka[4‡], Masao Ishimoto[4], Yasuo Yasui[3], Tetsuji Oya[2], Yasunari Fujita[1,5*]

[1] Biological Resources and Post-harvest Division, Japan International Research Center for Agricultural Sciences (JIRCAS); Tsukuba, Ibaraki 305-8686, Japan.
[2] Crop, Livestock and Environment Division, Japan International Research Center for Agricultural Sciences (JIRCAS); Tsukuba, Ibaraki 305-8686, Japan.
[3] Graduate School of Agriculture, Kyoto University; Kyoto, Kyoto 606-8502, Japan.
[4] Institute of Crop Science, National Agriculture and Food Research Organization (NARO); Tsukuba, Ibaraki 305-8518, Japan.
[5] Graduate School of Life Environmental Science, University of Tsukuba; Tsukuba, Ibaraki 305-8572, Japan.
[†]Present address: Institute of Crop Science, NARO; Tsukuba, Ibaraki 305-8518, Japan.
[‡]Present address: Center for Molecular Biodiversity Research, National Museum of Nature and Science; Tsukuba, Ibaraki 305-0005, Japan.

Yasunari Fujita[1,5*]

Biological Resources and Post-harvest Division, JIRCAS; 1-1 Ohwashi, Tsukuba, Ibaraki 305-8686, Japan.
[*]Corresponding author. E-mail: yasuf@affrc.go.jp

Abstract:
Drought severely damages crop production, even under conditions so mild that the leaves show no signs of wilting. As effective methods for analyzing the field drought response have not been established, it is unclear how field-grown plants respond to mild drought. We show that ridges are a useful experimental tool to mimic mild drought stress in the field. Mild drought reduces inorganic phosphate levels in the leaves to activate the phosphate starvation response (PSR) in field-grown soybean plants. PSR-related gene expression is mainly observed under drought conditions that are too mild to activate abscisic acid-mediated gene expression. Thus, our study provides insights into the molecular response to mild drought in field-grown plants and into the link between nutritional and drought stress responses in plants.

One-Sentence Summary:

Mimicking mild drought using ridges reveals that the phosphate response is a sign of drought reducing growth in plants.

Introduction:

Drought is a major threat to global crop production. Although tremendous progress has been made in deciphering the molecular mechanism of the drought stress response in model plants grown under controlled conditions (*1-3*), little is known about this mechanism in crops grown in the field, where conditions fluctuate and are difficult to predict and control. As a major oil and protein source for food, feed, biodiesel, and industrial products, soybean (*Glycine max* L. Merr.) is the most economically important dicot crop in the world (*4*). However, since soybean is cultivated mostly under rainfed conditions, soybean production is severely constrained by abiotic stresses, particularly drought (*5*). Even mild drought stress that occurs without obvious outward signs of a stress response such as leaf wilting poses a major threat to soybean productivity (*6*). Given that strategies to increase arable land area and yield face major obstacles, identifying ways to reduce crop production losses due to mild drought stress is a key goal in attaining global food security. However, since it is challenging to induce drought conditions to conduct experiments in the field due to uncontrollable weather, effective methods for analyzing the field drought response have not been developed. Here, using soybean as a model field-grown crop, we established that ridges could be used to induce conditions that mimic mild drought stress. We then used this system to explore the mechanisms underlying the plant's response to such conditions.

Results and Discussion:

Each growing season for six consecutive years, we created flat and ridged plots (referred to as "flats" and "ridges", respectively) to conduct mild drought tests in the field. We monitored the volumetric water content (VWC) of the soil using soil moisture sensors (Fig. 1, A and B, and figs. S1 to S3). In 2016, the soil VWC in the flats of our experimental field fluctuated between 34% (–170 kPa) and 49% (–4 kPa) (Fig. 1C and fig. S4). Although the VWC was strongly affected by rainfall (Fig. 1C), the VWC in ridges (ridge height, 30 cm; Fig. 1, A and B) was consistently lower than that of the flats and fluctuated between 27% (–530 kPa) and 41% (–44 kPa) (Fig. 1C and fig. S4). We compared the growth of soybean grown on the flats and ridges. The aboveground biomass of the plants grown on ridges was clearly reduced compared with that grown on flats, even though leaf wilting was not observed in either group of plants (Fig.

1D and fig. S5). Thermal image analysis of the soybean plants showed that the leaf temperature of the plants grown on ridges was higher than that of plants grown on flats (Fig. 1E), suggesting that transpiration was lower in the plants grown on ridges, which may have reduced the photosynthetic rate and biomass. Consequently, the yield of soybean grown on ridges was also reduced compared with that of soybean grown on flats (Fig. 1, F and G, fig S6). A decrease in transpiration and growth is a typical response of plants to water deficit, suggesting that growth on ridges induces mild drought stress in field-grown plants.

To ascertain whether the reduced growth of the plants grown on ridges was indeed due to water deficit or to changes in the nutrient composition of the soil, we measured the contents of nitrogen (N), phosphorous (P), and potassium (K) in the flats and ridges. There was no significant difference in the contents of these nutrients between the flats and ridges, both at the beginning and the end of the soybean growing season (Fig. 1H). We thus next examined whether watering the ridges would compensate for the negative effect of ridges on plant growth (Fig. 2 and fig. S7). In rainfed plants, there was a noticeable difference in soybean growth on flats and ridges, whereas in the irrigated plants, the difference was reduced or barely detectable (Fig. 2 and fig. S7, B to E). Thus, the negative effect of ridges on plant growth was complemented by irrigation, indicating that the reduced growth of the plants on ridges was mainly caused by water deficit. While a water deficit was not adequately induced on ridges in 2017, the results of the remaining five years of field trials demonstrated that the growth reduction of soybean on ridges compared to flats was a result of reduced VWC (Fig. 1 and figs. S7 to S9). Together, these observations demonstrate that ridges are a valuable tool to induce conditions that mimic mild drought stress.

To investigate how mild drought stress affects the expression of genes in field-grown soybean plants, we analyzed the fully expanded second trifoliate leaves of 29-day-old pre-flowering soybean plants in the 2015 field experiment by RNA sequencing (RNA-seq) (Fig. 3, A and B, fig. S9). We identified 3,045 differentially expressed genes (DEGs) between the soybean plants grown on flats and ridges (table S1), which had soil VWCs at sampling time of 41% (–26 kPa) and 34% (–123 kPa), respectively (figs. S4 and S9). We identified 990 and 400 DEGs that are up- and down-regulated ($|\log_2(FC)| \geq 1$, FPKM value > 0, $q < 0.05$), respectively, under mild drought conditions (Fig. 3C and tables S2 and S3). Gene ontology (GO) analysis (FDR < 0.05) revealed a total of 53 GO terms that were significantly enriched in up-regulated DEGs, while no GO terms were significantly enriched in down-regulated DEGs (table S4). Notably, 16 and 7 of the up-regulated DEGs were related to “cellular response to phosphate starvation” and “phosphate ion homeostasis”, respectively (fig. S10). Furthermore, 11.4% of the up-regulated DEGs were significantly enriched in phosphate starvation response (PSR)

106 family genes, including those encoding signaling factors, phosphatases, and transporters, and
107 in genes implicated in lipid metabolism, in *Arabidopsis thaliana* (*7*) and in soybean (*8*, *9*) (Fig.
108 3, D and E, and tables S5 and S6), indicating that a battery of PSR genes were up-regulated
109 under mild drought conditions. Mild drought stress tended to be induced the expression of PSR
110 marker genes in not only the second but also the first and third trifoliate leaves in the field-
111 grown soybean plants (Fig. 3F).

112 To determine whether reduced P levels are indeed observed under mild drought
113 conditions in the field, we determined the inorganic phosphate (Pi) concentration of the first to
114 third trifoliate leaves. The Pi concentrations in leaves at each of these positions in soybean
115 plants grown on ridges were significantly decreased compared with those grown on flats (Fig.
116 3G), indicating that mild drought stress decreases Pi levels in the leaves of field-grown soybean
117 plants. Our collective observations (Fig. 1, C and E, figs. S7 to S9) suggest that reduced
118 transpiration and water availability induced by mild drought inhibit Pi uptake by plants, leading
119 to Pi deficiency conditions. Combined with a previous meta-analysis using various plants and
120 soil types (*10,11*) and physiological experiments with soybean grown in pots (*12*), these
121 observations support the notion that mild drought stress reduces Pi levels to induce the PSR in
122 field-grown plants.

123 We next explored if the link between mild drought stress and the PSR identified in
124 our field experiments could be reproduced in pot trials (Fig. 4). When the primary soybean
125 leaves were fully expanded at 10 days after sowing in pots containing the same soil as that used
126 in the field experiments, we started the drought stress treatments with five different levels of
127 VWC, α to ε (increasing water deficit; Fig. 4A). The leaf surface temperatures of 26-day-old
128 soybean plants visualized by infrared thermography paralleled the soil VWCs in the pots (Fig.
129 4, A and B), suggesting that the lower the VWC, the greater the reduction in transpiration under
130 the experimental condition. We analyzed the gene expression profiles of the fully expanded
131 first trifoliate leaves of 38-day-old seedlings grown in pots. The expression levels of PSR genes
132 were largely inversely associated with VWC levels of α to δ, but not ε (Fig. 4C). Thus, the soil
133 water status determines the degree of the PSR under mild drought stress conditions, supporting
134 the findings of our field experiments. Interestingly, between pots δ and ε, even though the
135 VWC decreased, PSR gene expression did not increase, but the expression of abscisic acid
136 (ABA)-responsive genes, which are established markers of the response to severe drought
137 stress (*13,14*), did increase (Fig. 4, C and D). Thus, the PSR, and not ABA, is an important
138 indicator of mild drought stress in the field (Fig. 4E).

139 Here, we reveal a novel link between the PSR and drought response in plants. This
140 insight was possible because the experiments were conducted in an actual field, where available

P is not abundant and P acquisition is dependent on the biotic and abiotic environment (*15*). While ridges are widely used in crop production for various purposes, they have not been used to explore the drought response in plants. Our research using ridges provides insight into the link between plant nutritional and drought stress responses and paves the way for elucidating the molecular mechanism of the drought response in field-grown plants. Since it is easy and inexpensive to create ridges in experimental fields, this method of inducing mild drought stress overcomes a major research barrier, and is expected to facilitate efforts around the world aimed at deciphering the response of field-grown crops to various degrees of drought stress. Global food security depends on producing crops that can maintain productivity even under mild to moderate soil water deficits (*16*, *17*). The PSR could be used as an early marker of mild drought stress, allowing irrigation to be optimized before the yield of field-grown crops is affected by mild drought conditions.

Materials and Methods:

Field experiment

Soybean (*Glycine max* L. Merr.) cv. Williams 82, a sequenced model US cultivar (*18*), was used in this study for all years other than 2019. Soybean cv. Enrei, a sequenced model Japanese cultivar (*19*), was used only in the 2019 field experiment. Field experiments were conducted at the experimental field at the Japan International Research Center for Agricultural Sciences (JIRCAS, 36°03′14″ N, 140°04′46″ E, 24 m above sea level) located in Ibaraki, Japan, from 2015 to 2020. The soil type is Andosol (*20*) and the site has a typical temperate climate. In the experimental field, no fertilizers have been applied. To mimic mild drought stress in the experimental field, we created ridges with a tiller coupled to a rotary after plowing (fig. S1A). In field trials conducted in the 2015–2018 growing seasons, the ridges were produced with a TA6 or TA800N tiller (Kubota, Osaka, Japan) coupled to an RA3 rotary (Kubota) and were 30 cm high and 38 cm wide at the base. In the 2019 and 2020 growing seasons, since the same size rotary was unavailable, ridges were created using a TA800N tiller (Kubota) coupled to a SKB-E15C rotary (Kubota) and were 30 cm high and 63 cm wide at the base. Because the thickness of A horizon, a topsoil characterized by organic matter accumulation, is greater than 30 cm in our experimental field, both the flat and ridged plots were composed of this topsoil.

In 2015, the experimental layout consisted of two areas with flat and ridged plots (fig. S2A). In each area, three plots were used for the analysis. Soybean seeds were sown at 20-cm intervals on August 3, and a total of 30 plants were grown per plot. For 5 days after sowing, water was sprayed every day to prompt seed germination. In 2016, the experiment was laid out in a randomized complete block design, including flat and ridged plots, with four blocks for

176 four replicates (fig. S2B). Soybean seeds were germinated on vermiculite in a temperature-
177 controlled phytotron at JIRCAS (27 ± 6 °C), as described previously (*21*), on July 7, and 30
178 healthy and uniform 6-day-old seedlings were planted per plot at 20-cm intervals on July 13.
179 In 2017, the experimental layout was divided into two areas, one irrigated and the other rainfed.
180 Each area was composed of randomized blocks, including flat and ridged plots, with four
181 replicates (fig. S3A). In the irrigated area, irrigation tubes (EVAFLOW, Mitsubishi Chemical
182 Agri Dream, Tokyo, Japan) were installed to supply water to the entire area of each plot.
183 Soybean seeds were sown at 20-cm intervals on July14, and a total of 15 plants were grown
184 per plot. To avoid drought stress for seedling establishment, all plots were surrounded by
185 irrigation tubes and irrigated a total of four times from the day before sowing to 7 days after
186 sowing. Subsequently, the irrigated area was irrigated 20 times during the period from 18 to 95
187 days after sowing. Too much irrigation may have increased soil moisture throughout the test
188 area and failed to induce adequate water deficit on ridges (fig. S8A). In 2018, the experimental
189 layout consisted of two areas, one irrigated and the other rainfed (fig. S2C). Each area included
190 randomized blocks, with flat and ridged plots, and with four replicates. In the irrigated area,
191 each plot was surrounded by irrigation tubes and irrigated 9 times during the period from 15 to
192 53 days after sowing (fig. S7A). Soybean seeds were sown at 20-cm intervals on July 19, and
193 a total of 25 plants were grown per plot. In 2019, the experiment was laid out in a randomized
194 complete block design, including flat and ridged plots, with four blocks for four replicates (fig.
195 S3B). Seeds were germinated on vermiculite in a temperature-controlled phytotron (27 ± 6°C)
196 on July 12, and 20 healthy and uniform 6-day-old seedlings were planted per plot at 20-cm
197 intervals. In 2020, the experimental layout consisted of two areas, one irrigated and the other
198 rainfed (fig. S3C). Each area included randomized blocks, with flat and ridged plots, and with
199 four replicates. In the irrigated area, each plot was surrounded by irrigation tubes and irrigated
200 only once, at 28 days after sowing (fig. S8C). Seeds were germinated on vermiculite in a
201 temperature-controlled phytotron (27 ± 6 °C) on July 30, and 25 healthy and uniform seedlings
202 were planted per plot at 20-cm intervals on August 6.
203
204 **Pot experiment**
205 Pot experiments were conducted in a greenhouse (20 ± 10°C) at JIRCAS to examine how the
206 soil volumetric water content (VWC) affects phosphate starvation response (PSR)-related gene
207 expression in soybean. Soybean seeds were germinated on moistened vermiculite in a
208 temperature-controlled phytotron (*21*) and then the five-day-old seedlings were transferred to
209 350 ml pots filled with A horizon collected from the JIRCAS experimental field. The seedlings
210 were grown under well-watered conditions (up to a VWC of 43%) for five days in the

211 greenhouse. When primary leaves were fully expanded at 10 days after sowing, we started to
212 adjust the VWC to five different levels, α (42–57%), β (35–50%), γ (30–43%), δ (24–36%),
213 and ε (20–29%), by measuring the weight of the pot, adding water every Monday, Wednesday,
214 and Friday. The fully expanded first trifoliate leaves of 38-day-old seedlings were collected
215 and immediately frozen in liquid nitrogen. Then, the total RNA from leaves was used for gene
216 expression analysis.
217
218 **Meteorological data**
219 Meteorological data, such as amount of rainfall, were obtained from the Weather Data
220 Acquisition System of Institute for Agro-Environmental Sciences, National Agriculture and
221 Food Research Organization (http://www.naro.affrc.go.jp/org/niaes/aws/). The weather station
222 is located at 36°01′ N, 140°07′ E, approximately 5 km from the JIRCAS experimental field.
223
224 **Evaluation of growth and yield performance of soybean in the field**
225 To investigate the effect of mild drought stress induced by ridges on soybean growth, we
226 measured the aboveground biomass at three time points per growing season in 2015 and 2016.
227 In 2015, a total of 5 plants (1 or 2 plants per plot), 7 plants (2 or 3 plants per plot), and 7 plants
228 (2 or 3 plants per plot) were selected randomly to measure the aboveground biomass at 21, 30,
229 and 44 days after sowing, respectively. In 2016, a total of 12 plants (3 plants per plot) were
230 selected randomly for measurements of aboveground biomass at 20, 36, and 50 days after
231 sowing. Dry weight of the aboveground biomass was measured after oven-drying at 65°C for
232 more than 48 h.
233 We evaluated the yield of soybean plants in field trials during 2015–2020. In 2015, a
234 total of 11 plants (3–4 plants per plot) grown on the flat plots and 12 plants (4 plants per plot)
235 grown on the ridged plots were selected randomly and harvested on December 1. The number
236 of seeds per plant and total air-dried seed weight per plant were measured. In 2016, a total of
237 20 plants (5 plants per plot) for each condition were selected and harvested on November 10.
238 After oven-drying at 65°C for more than 48 h, we measured the following parameters for each
239 plant: number of seeds, total seed weight, stem weight, and pod-shell weight. The harvest index
240 was calculated as total seed weight / (total seed weight + stem weight + pod-shell weight). In
241 2017, a total of 24 plants (6 plants per plot) were selected randomly for each treatment and
242 harvested on November 15. After oven-drying at 65°C for more than 48 h, we measured the
243 following parameters for each plant: number of seeds, total seed weight, combined stem and
244 pod-shell weight, and plant height. In 2018, a total of 48 plants (12 plants per plot) were
245 selected randomly for each treatment and harvested on November 14. After oven-drying at

65°C for more than 48 h, we measured the following parameters for each plant: number of seeds, total seed weight, stem and pod-shell weight, plant height, and total branch length. In 2019, a total of 40 plants (10 plants per plot) were selected randomly for each treatment and harvested on November 13. Since soybean plants were damaged by a typhoon on September 8, we measured only the total biomass, including seeds, stem, and pod shell as preliminary data. In 2020, a total of 40 plants (10 plants per plot) were selected randomly for each treatment and harvested on November 2. After oven-drying at 65°C for more than 48 h, we measured the following parameters for each plant: total seed weight and combined stem and pod-shell weight.

Image acquisition

Thermal images of soybean plants were taken using a thermal imaging infrared camera (CPA-T640A, CHINO, Tokyo, Japan) according to the manufacturer's protocol. Aerial images of the experimental field were obtained using an unmanned aerial vehicle (Phantom 4, DJI, Shenzhen, China) according to the manufacturer's protocol.

Measurements of soil water contents

Based on the preliminary investigation of soybean roots in the flat and ridged plots in this experimental field of JIRCAS, we decided to measure the soil moisture content at 0–20 cm or 0–30 cm, starting from the top of the ridge or the flat, in this study. In 2015, the volumetric water content (VWC, $m^3\ m^{-3}$) at a depth of 0–20 cm was measured in each experimental plot at intervals of about 3 days with a 20-cm-long time domain reflectometry (TDR) probe (Hydrosense II, Campbell Scientific Inc., Logan, UT, USA). Then, *in situ* calibration was conducted using the gravimetric method according to the manufacturer's protocol. The tentative values of VWCs were measured using the TDR probe, and the soils at the measured sites were collected from a depth of 0–20 cm with polyvinyl chloride pipes (4.3 cm in diameter and 20 cm in length). Soil weights including water were determined. After pre-drying at 60°C for more than 24 h, soil samples were removed from the pipes and oven-dried at 105°C for more than 24 h to calculate the gravimetric water content ($g\ g^{-1}$). A total of eight points were measured on any four days. Then, the gravimetric water content was converted into VWC by multiplying it by the bulk density (BD, $Mg\ m^{-3}$), assuming that the water density is 1.0 $Mg\ m^{-3}$. Since Andosols generally have a high porosity (*22*) (about 70% in this study) and can be easily compressed, it was difficult to collect an accurate volume of a soil from a depth of 0–20 cm using a single pipe in the field. Therefore, to determine the BD of soils from a depth of 0–20 cm, we carefully collected soil samples from a depth of 10–15 cm using 100-ml soil sampling cores (DIK-1801-11, Daiki Rika Kogyo, Konosu, Japan) at 12 points, and then

determined the dry wights of the 100-ml soil sample after oven-drying at 105°C for more than 48 h. The average BD of soils from a depth of 0–20 cm was 0.734 ± 0.017 (mean ± SD) Mg m^{-3}. From the relationships between the tentative values of VWCs recorded by the TDR probe (estimated value) and those determined *in situ* (true value), we obtained a calibration formula: actual VWC = 0.9718 × tentative VWC + 12.554.

In 2016–2020, the VWC at a depth of 0–30 cm was automatically recorded in each plot every day at 10:00 a.m. with a 30-cm-long TDR probe (CS616, Campbell Scientific, Inc.) connected to a data logger (CR1000, Campbell Scientific, Inc.). Soil temperature at a depth of 12–18 cm was also recorded with a temperature probe (107, Campbell Scientific, Inc.) to correct for the temperature dependence of the TDR probes, according to the manufacture's protocol. The estimated VWCs recorded by the TDR probes were similarly calibrated using the gravimetric method according to the manufacture's protocol. We selected eight TDR probes for the calibration and inserted the probes into a plot with temperature probes in the experimental field. The soil samples were collected from four points of the plot on any seven days, yielding a total of 28 soil samples, with polyvinyl chloride pipes (4.3 cm in diameter and 30 cm in length), and then the soil weight was determined. The dry weights of the soil samples were determined as described above. We measured the BD at a depth of 0–10 cm and 10–30 cm to determine the BD at a depth of 0–30 cm, because the BD differed at each depth under our test conditions in the field. To determine the BD of soils at a depth of 0–30 cm, we carefully collected soil samples from depths of 3–8 cm and 20–25 cm using the 100 ml soil sampling cores (DIK-1801-11, Daiki Rika Kogyo) at 8 points each. The BD for depths of 0–30 cm was determined to be 0.773 Mg m^{-3} by the combined weighted average of the values obtained for depths of 0–10 cm and 10–30 cm. According to the manufacture's protocol, the output period data of each TDR probe at the sampling times were corrected by temperature, and the tentative VWCs were calculated. Using the averages of tentative values of VWCs obtained using the eight probes and the corresponding actual VWCs determined *in situ* at each sampling point, we generated a calibration formula: actual VWC = 1.0005 × tentative VWC + 0.1514.

Measurements of soil nutrients

Soil samples were taken from a depth of about 0–30 cm with a polyvinyl chloride cylinder or soil sampler (DIK-1601, Daiki Rika Kogyo) in each plot on July 7 and November 17, 2016, which corresponded to the start and end of the soybean cultivation period, respectively. Samples were air-dried and passed through a 2–mm sieve. Then, the obtained fine earth was subjected to soil chemical analysis. The oven-dried weight of the fine earth was measured to

obtain the moisture correction factors that were used to convert nutrient contents on air-dried soil to a dry weight basis.

Total carbon and total nitrogen contents were determined using the dry combustion method with an elemental analyzer (Sumigraph NC-220F, Sumika Chemical Analysis Service, Tokyo, Japan). Exchangeable bases (K^+) extracted in 1 M ammonium acetate (pH 7) were measured basically as described previously (*23*), except that inductively coupled plasma atomic emission spectroscopy with a spectrometer (ICPE-9000, Shimadzu Corporation, Kyoto, Japan) was used in this study. Available phosphorus was determined using the Bray-II method (*24*) with a spectrophotometer (UV-1800, Shimadzu Corporation).

Soil water retention curve

Soil samples were collected from a depth of 10–15 cm using 100-ml soil sampling cores (DIK-1801-11, Daiki Rika Kogyo) at six points in each plot. The soil water retention, a relationship between the VWC (θ) and soil water potential (ψ), of each sample was measured with a pressure plate apparatus at a water potential of between –3.9 kPa and –98 kPa, as described previously (*25*), and with a dew point potentiometer (WP4, Decagon Devices, Pullman, WA, USA) at values below –310 kPa, as described previously (*26*). The values of VWCs at a depth of 0–20 cm and 0–30 cm were calculated using the BD values at each depth. The averaged VWCs are shown at matric potential values of –3.9, –9.8, –31, –98, –619, and –1554 kPa (fig. S4). Both regression curves at a depth of 0–20 cm and 0–30 cm were obtained by fitting a hydraulic model (*27*) using SWRC Fit (*28*):

$$\theta = \theta_s \left[\frac{1}{\ln[e + (\psi/a)^n]}\right]^m$$

where θ_s is the saturated VWC; e is the Napier's constant; and a, n, and m are three different soil parameters. The model showed a good fit (R^2=0.985, $p < 0.001$ for both curves).

Transcriptome analysis

A total of 10 plants (3 or 4 plants per plot) were randomly selected from each treatment group, and the first to third trifoliate leaves were collected individually and immediately frozen in liquid nitrogen in the field on September 1, 2015. The frozen second trifoliate leaves were powdered using a multi-bead shocker (YASUI KIKAI, Osaka, Japan) and the other leaves were powdered using a mortar and pestle. For RNA-seq analysis, total RNA was extracted from powdered samples of fully expanded second trifoliate leaves using an RNeasy Plant Mini Kit (Qiagen, Hilden, Germany) following the manufacturer's protocol. The extracted total RNA samples from three independent plants per plot were mixed for one replicate, and in total three

349 biological replicates were performed in each treatment. The extracted RNA was used to
350 construct paired-end libraries using a TruSeq RNA Library Preparation Kit v2 (Illumina, CA,
351 USA). The libraries were sequenced on an Illumina HiSeq 4000 sequencer with a 100-bp
352 paired-end protocol (Macrogen, Kyoto, Japan). For trimming low quality reads and adaptor
353 sequences, a Trimmomatic v0.36 (*29*) with the option of SLIDINGWINDOW:4:20,
354 MINLEN:40, LEADING:20, and TRAILING:20 was used. The trimmed reads were mapped
355 against the reference sequence of Williams 82 (Wm82.a2.v1:
356 https://phytozome.jgi.doe.gov/pz/portal.html) using STAR v2.5.1 (*30*) with the option of
357 outSJfilterReads: Unique; outFilterMatchNminOverLread: 0.96; and
358 outFilterScoreMinOverLread: 0.8. The FPKM (fragment per kilobase of exon per million
359 mapped reads) of each gene was calculated using Cufflinks v2.2.1 (*31*). Differential expression
360 analysis was performed by Cuffdiff embedded in Cufflinks v2.2.1 (*31*). The genes that showed
361 q value < 0.05 were defined as differentially expressed genes (DEGs) between the samples
362 grown on flat and ridged plots. Gene annotation such as homology to *Arabidopsis thaliana*
363 genes and GO was obtained from gene annotation information in Wm82.a2.v1
364 (Gmax_275_Wm82.a2.v1.annotation_info.txt).
365 A heatmap of up- and down-regulated DEGs was constructed with the 'heatmap.2'
366 function of the gplots package in R software v3.3.3 (*32*). The different types of representative
367 phosphate starvation responsive genes were selected in the up-regulated genes based on a
368 previous report (*7*). Using the clusterProfiler package in R (*33*), GO enrichment analysis was
369 performed for the up- and down-regulated DEGs selected according to the following criteria:
370 $|\log_2(FC)| \geq 1$, FPKM value > 0, $q < 0.05$. A directed acyclic graph (DAG) was constructed
371 using the clusterProfiler package in R. FDR < 0.05 was regarded as significantly enriched GO
372 terms. The GO descriptions were obtained using AnnotationHub ("AH13355") in R (*34*). We
373 assessed the significant enrichment of PSR marker genes (*7-9*) in the up- and down-regulated
374 genes using the hypergeometric tests (phyper function in R).
375
376 **RT-qPCR analysies**
377 For RT-qPCR analysis, total RNA was extracted from soybean leaves using an RNeasy Plant
378 Mini Kit (Qiagen) or RNAiso Plus (Takara Bio, Kusatsu, Japan) according to the
379 manufacturer's protocol. The extracted total RNA was treated with RQ1 RNase-free DNase
380 (Promega, Madison, WI, USA). Complementary DNA (cDNA) was synthesized using
381 PrimeScript RT Master Mix (Takara Bio). RT-qPCR using GoTaq qPCR Master Mix
382 (Promega) was performed by QuantStudio7 Flex (Applied Biosystems, Foster City, CA, USA).
383 The relative amounts of target mRNAs were calculated using the relative standard curve

method and normalized against actin (*Glyma.15G050200*) as a reference gene. The primers used in this study are listed in Supplementary Table S7.

Measurements of inorganic phosphate contents

We examined the inorganic phosphate (Pi) contents in soybean leaves using a molybdate colorimetric assay (*35,36*). The frozen powdered leaf samples used for gene expression analysis were used to analyze the Pi content. A total of 20–45 mg of each sample was mixed with 1% acetic acid (20 µl/mg sample weight), vortexed for 15 min, and incubated at 42°C for 1 h in a heat block. Following centrifugation at 18,300 g for 5 min at room temperature, the supernatant was used for the Pi assay. Reaction solutions containing 140 µl of molybdate solution (a master mix of a 6:1 proportion of 0.42% (w/v) ammonium molybdate in 1 N H_2SO_4 and 10% ascorbic acid in water) and 60 µl of the supernatants were incubated in a 96-well plate at 42°C for 20 min using a thermal cycler. The absorbance of 100 µl of the reaction solutions at 820 nm was measured using a plate reader (ARVOX3, PerkinElmer, MA, USA). The amount of Pi in the solution was calculated using a calibration curve diluted based on Phosphorus Standard Solution (FUJIFILM Wako, Osaka, Japan).

Statistical analysis

Statistical tests in this study, except for the hypergeometric enrichment analysis of PSR (Fig. 3D) conducted by the R function "phyper", were performed in GraphPad Prism 9 (GraphPad software, La Jolla, CA, USA). An unpaired, two-tailed *t*-test or a one-way analysis of variance (ANOVA) with Tukey's test was used in most experiments. The data shown in Fig. 2 and Fig. S7 did not seem to be homoscedastic. Therefore, Brown-Forsythe and Welch ANOVA tests with a Dunnett's T3 multiple comparisons test were used.

References and Notes:

1. J-K. Zhu, Abiotic stress signaling and responses in plants. *Cell* **167**, 313−324 (2016). doi: 10.1016/j.cell.2016.08.029; pmid: 27716505
2. M. Dubois, D. Inzé, Plant growth under suboptimal water conditions: early responses and methods to study them. *J. Exp. Bot.* **71**, 1706−1722 (2020). doi: 10.1093/jxb/eraa037; pmid: 31967643
3. H. Claeys, D. Inzé, The agony of choice: how plants balance growth and survival under water-limiting conditions. *Plant Physiol.* **162**, 1768−1779 (2013). doi: 10.1104/pp.113.220921; pmid: 23766368

418 4. P. H. Graham, C. P. Vance, Legumes: importance and constraints to greater use. *Plant*
419 *Physiol.* **131**, 872−877 (2003). doi: 10.1104/pp.017004; pmid: 12644639
420 5. L. P. Manavalan, S. K. Guttikonda, L.-S. P. Tran, H. T. Nguyen, Physiological and molecular
421 approaches to improve drought resistance in soybean. *Plant Cell Physiol.* **50**, 1260−1276
422 (2009). doi: 10.1093/pcp/pcp082; pmid: 19546148
423 6. M. G. Gebre, H. J. Earl, Soil water deficit and fertilizer placement effects on root biomass
424 distribution, soil water extraction, water use, yield, and yield components of soybean
425 [*Glycine max* (L.) Merr.] grown in 1-m rooting columns. *Front. Plant Sci.* **12**, 581127 (2021).
426 doi: 10.3389/fpls.2021.581127; pmid: 33790918
427 7. G. Castrillo, P. J. P. L. Teixeira, S. H. Paredes, T. F. Law, L. de Lorenzo, M. E. Feltcher, O.
428 M. Finkel, N. W. Breakfield, P. Mieczkowski, C. D. Jones, J. Paz-Ares, J. L. Dangl, Root
429 microbiota drive direct integration of phosphate stress and immunity. *Nature* **543**, 513−518
430 (2017). doi: 10.1038/nature21417; pmid: 28297714
431 8. C. Li, S. Gui, T. Yang, T. Walk, X. Wang, H. Liao, Identification of soybean purple acid
432 phosphatase genes and their expression responses to phosphorus availability and symbiosis.
433 *Ann. Bot.* **109**, 275−285 (2012). doi: 10.1093/aob/mcr246; pmid: 21948626
434 9. Z. Yao, J. Tian, H. Liao, Comparative characterization of GmSPX members reveals that
435 GmSPX3 is involved in phosphate homeostasis in soybean. *Ann. Bot.* **114**, 477−488 (2014).
436 doi: 10.1093/aob/mcu147; pmid: 25074550
437 10. L. D. B. Suriyagoda, M. H. Ryan, M. Renton, H. Lambers, Plant responses to limited
438 moisture and phosphorus availability: a meta-analysis. *Adv. Agron.* **124**, 143–200 (2014).
439 doi: 10.1016/B978-0-12-800138-7.00004-8
440 11. M. He, F. A. Dijkstra, Drought effect on plant nitrogen and phosphorus: a meta-analysis.
441 *New Phytol.* **204**, 924−931 (2014). doi: 10.1111/nph.12952; pmid: 25130263
442 12. D. T. Krizek, A. Carmi, R. M. Mirecki, F. W. Snyder, J. A. Bunce, Comparative effects of
443 soil moisture stress and restricted root zone volume on morphogenetic and physiological
444 responses of soybean [*Glycine max* (L.) Merr.]. *J. Exp. Bot.* **36**, 25−38 (1985). doi:
445 10.1093/jxb/36.1.25
446 13. Y. Fujita, M. Fujita, K. Shinozaki, K. Yamaguchi-Shinozaki, ABA-mediated
447 transcriptional regulation in response to osmotic stress in plants. *J. Plant Res.* **124**, 509−525
448 (2011). doi: 10.1007/s10265-011-0412-3; pmid: 21416314
449 14. L. Song, S. C. Huang, A. Wise, R. Castanon, J. R. Nery, H. Chen, M. Watanabe, J. Thomas,
450 Z. Bar-Joseph, J. R. Ecker, A transcription factor hierarchy defines an environmental stress
451 response network. *Science*. **354**, aag1550 (2016). doi: 10.1126/science.aag1550. pmid:
452 27811239

15. J. Pang, M. H. Ryan, H. Lambers, K. H. M. Siddique, Phosphorus acquisition and utilisation in crop legumes under global change. *Curr. Opin. Plant Biol.* **45**, 248−254 (2018). doi: 10.1016/j.pbi.2018.05.012; pmid: 29853281
16. F. Tardieu, Any trait or trait-related allele can confer drought tolerance: just design the right drought scenario. *J. Exp. Bot.* **63**, 25−31 (2012). doi: 10.1093/jxb/err269; pmid: 21963615
17. F. Tardieu, T. Simonneau, B. Muller, The physiological basis of drought tolerance in crop plants: A scenario-dependent probabilistic approach. *Annu. Rev. Plant Biol.* **69**, 733−759 (2018). doi: 10.1146/annurev-arplant-042817-040218; pmid: 29553801
18. J. Schmutz, S. B. Cannon, J. Schlueter, J. Ma, T. Mitros, W. Nelson, D. L. Hyten, Q. Song, J. J. Thelen, J. Cheng, D. Xu, U. Hellsten, G. D. May, Y. Yu, T. Sakurai, T. Umezawa, M. K. Bhattacharyya, D. Sandhu, B. Valliyodan, E. Lindquist, M. Peto, D. Grant, S. Shu, D. Goodstein, K. Barry, M. Futrell-Griggs, B. Abernathy, J. Du, Z. Tian, L. Zhu, N. Gill, T. Joshi, M. Libault, A. Sethuraman, X.-C. Zhang, K. Shinozaki, H. T. Nguyen, R. A. Wing, P. Cregan, J. Specht, J. Grimwood, D. Rokhsar, G. Stacey, R. C. Shoemaker, S. A. Jackson, Genome sequence of the palaeopolyploid soybean. *Nature* **463**, 178–183 (2010). doi: 10.1038/nature08670; pmid: 20075913
19. M. Shimomura, H. Kanamori, S. Komatsu, N. Namiki, Y. Mukai, K. Kurita, K. Kamatsuki, H. Ikawa, R. Yano, M. Ishimoto, A. Kaga, Y. Katayose, The *Glycine max* cv. Enrei genome for improvement of Japanese soybean cultivars. *Int. J. Genomic.* **2015**, 358127 (2015). doi: 10.1155/2015/358127; pmid: 26199933
20. IUSS Working Group WRB, "World reference base for soil resources 2014, update 2015" (World Soil Resources Rep. Vol. 106, Food and Agriculture Organization of the United Nations, 2015; http://www.fao.org/3/i3794en/I3794en.pdf)
21. Y. Nagatoshi, Y. Fujita, Accelerating soybean breeding in a CO_2-supplemented growth chamber. *Plant Cell Physiol.* **60**, 77–84 (2019). doi: 10.1093/pcp/pcy189; pmid: 30219921
22. P. Driessen, J. Deckers, O. Spaargaren, F. Nachtergaele, Eds., "Andosols" in *Lecture Notes on the Major Soils of the World* (World Soil Resources Rep. Vol. 94, Food and Agriculture Organization of the United Nations, 2001; http://www.fao.org/3/y1899e/y1899e.pdf).
23. L. P. Van Reeuwijk, "Procedures for Soil Analysis" (Tech. Paper Vol. 9, International Soil Reference and Information Centre (ISRIC), Wageningen, 2002; https://www.isric.org/sites/default/files/ISRIC_TechPap09.pdf).
24. R. H. Bray, L. T. Kurtz, Determination of total, organic, and available forms of phosphorus in soils. *Soil Sci.* **59**, 39–46 (1945). doi: 10.1097/00010694-194501000-00006
25. J. H. Dane, J. W. Hopmans, "Pressure plate extractor" in *Methods of Soil Analysis*, J. H. Dane, G. C. Topp, Eds. (SSSA, Madison, 2002), Part 4: Physical methods, pp. 688–690.

26. B. R. Scanlon, B. J. Andraski, J. Bilskie, "*Dew point potentiameter*" in Methods of soil analysis, Part 4: Physical methods, J. H. Dane, G. C. Topp, Eds. (SSSA, Madison, 2002) pp. 662–665.
27. D. G. Fredlund, A. Xing, Equations for the soil-water characteristic curve. *Can. Geotech. J.* **31**, 521–532 (1994). doi: doi.org/10.1139/t94-061
28. K. Seki, SWRC fit – a nonlinear fitting program with a water retention curve for soils having unimodal and bimodal pore structure, *Hydrol. Earth Syst. Sci. Discuss.* **4**, 407–437 (2007). doi: 10.5194/hessd-4-407-2007
29. A. M. Bolger, M. Lohse, B. Usadel, Trimmomatic: a flexible trimmer for Illumina sequence data. *Bioinformatics* **30**, 2114–2120 (2014). doi: 10.1093/bioinformatics/btu170; pmid: 24695404
30. A. Dobin, C. A. Davis, F. Schlesinger, J. Drenkow, C. Zaleski, S. Jha, P. Batut, M. Chaisson, T. R. Gingeras, STAR: ultrafast universal RNA-seq aligner. *Bioinformatics* **29**, 15–21 (2013). doi: 10.1093/bioinformatics/bts635; pmid: 23104886
31. C. Trapnell, B. A. Williams, G. Pertea, A. Mortazavi, G. Kwan, M. J. van Baren, S. L. Salzberg, B. J. Wold, L. Pachter, Transcript assembly and quantification by RNA-Seq reveals unannotated transcripts and isoform switching during cell differentiation. *Nat. Biotechnol*. **28**, 511–515 (2010). doi: 10.1038/nbt.1621; pmid: 20436464
32. G. R. Warnes, B. Bolker, L. Bonebakker, R. Gentleman, W. Huber, A. Liaw, T. Lumley, M. Maechler, A. Magnusson, S. Moeller, M. Schwartz, B. Venables, T. Galili, gplots: Various R programming tools for plotting data, 2016. https://cran.r-project.org/web/packages/gplots/index.html
33. G. Yu, L. G. Wang, Y. Han, Q. Y. He, clusterProfiler: an R package for comparing biological themes among gene clusters. *OMICS* **5**, 284–287 (2012). doi: 10.1089/omi.2011.0118; pmid: 22455463
34. M. Morgan, M. Carlson, D. Tenenbaum, S. Arora, AnnotationHub: Client to access AnnotationHub resources. R package version 2.10.1., 2017. doi: 10.18129/B9.bioc.AnnotationHub
35. B. N. Ames, Assay of inorganic phosphate, total phosphate and phosphatases. *Methods Enzymol.* **8**, 115–118 (1966). doi: 10.1016/0076-6879(66)08014-5
36. T. J. Chiou, K. Aung, S.-I. Lin, C. C. Wu, S.-F. Chiang, C.-L. Su, Regulation of phosphate homeostasis by MicroRNA in *Arabidopsis*. *Plant Cell* **18**, 412–421 (2006). doi: 10.1105/tpc.105.038943; pmid: 16387831

Acknowledgments: We thank S. Shu, M. Toyoshima, K. Ozawa, K. Shimizu, N. Hisatomi, Y. Saito, J. Baba, M. Ohsaki, Y. Shirai, Y. Nakamura, I. Gejima, H. Ohwada, N. Tayama, K. Kawamura, T. Komatsu, and H. Ishiyama for technical assistance; and T. Taji, K. Nakashima, M. Fujita, and T. Ogata for discussions.

Funding: This work was supported by the Grants-in-Aid for Scientific Research (KAKENHI) by the Japan Society for the Promotion of Science (JSPS) (Grant Nos. JP18K05379 to YN; JP21H02158 to YN, YF; JP16K07412, JP24510312 to YF), Cross-ministerial Moonshot Agriculture, Forestry and Fisheries Research and Development Program by the Bio-oriented Technology Research Advancement Institution (BRAIN) (Grant No. JPJ009237), the Science and Technology Research Partnership for Sustainable Development (SATREPS) by the Japan Science and Technology Agency (JST) and the Japan International Cooperation Agency (JICA) (Grant No. JPMJSA1907), and the Ministry of Agriculture, Forestry and Fisheries (MAFF) of Japan.

Author contributions: Y.N. and Y.F. conceived and designed the study and wrote the paper; Y.N. performed most of the experiments and analyzed the data; K.I. performed the soil and chemical analyses; Y.N., K.F., and Y.F. performed the field experiments, with support from T.O. and Y.K.; Y.N., N.M., Y.K., E.O-T., M.I., and Y.Y. performed the transcriptome analysis. All authors discussed and commented on the manuscript.

Competing interests: The authors declare no competing interests.

Data and materials availability: RNA-seq data are available from the DNA Data Bank of Japan (www.ddbj.nig.ac.jp/) under accession number DRA012279. No restrictions are placed on materials, such as materials transfer agreements. Details of all data, code, and materials used in the analysis are available in the main text or the supplementary materials.

Supplementary Materials

Figs. S1 to S10

Tables S1 to S7

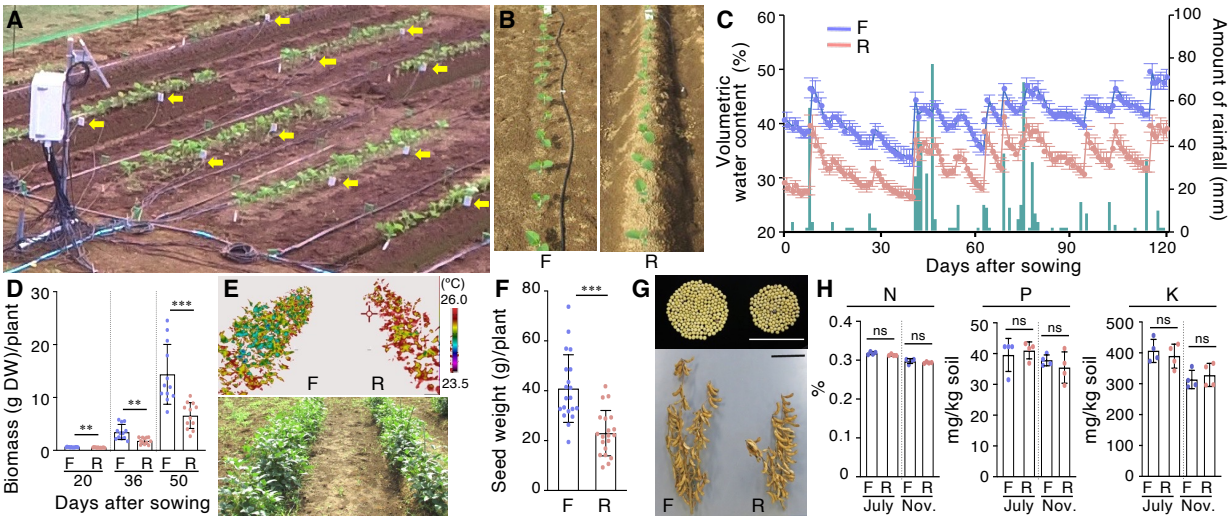

Fig. 1. Ridges can artificially induce mild drought stress, reducing soybean yield. (**A**) Photograph of the experimental field, including the VWC data collection station, watering tubes, and probes (yellow arrows). (**B**) Twelve-day-old soybean plants on flat and ridged plots (referred to as "flats" and "ridges", respectively). (**C**) Daily rainfall (dark green bars) and time-course of soil VWC ($n = 4$) in the flats (blue lines and points) and ridges (pink lines and points) over the study period in the 2016 field. (**D**) Aboveground biomass (dry weight, DW) per plant grown on the flats and ridges ($n = 12$). F and R denote flats and ridges, respectively. (**E**) Thermogram and the corresponding digital image of 9-week-old soybean plants grown on the flats and ridges in 2016. (**F**) Total seed weight per plant grown on the flats and ridges ($n = 20$). (**G**) Seeds from individual representative plants grown on the flats and ridges. Scale bars, 10 cm. (**H**) Nutrient contents (N, P, and K) of soil in the flats and ridges before (July) and after (November) soybean cultivation in 2016 ($n = 4$). $^{**}P < 0.01$, $^{***}P < 0.001$; Student's *t*-test; ns, no significant difference. Error bars in (C), (D), (F), and (H) denote SD.

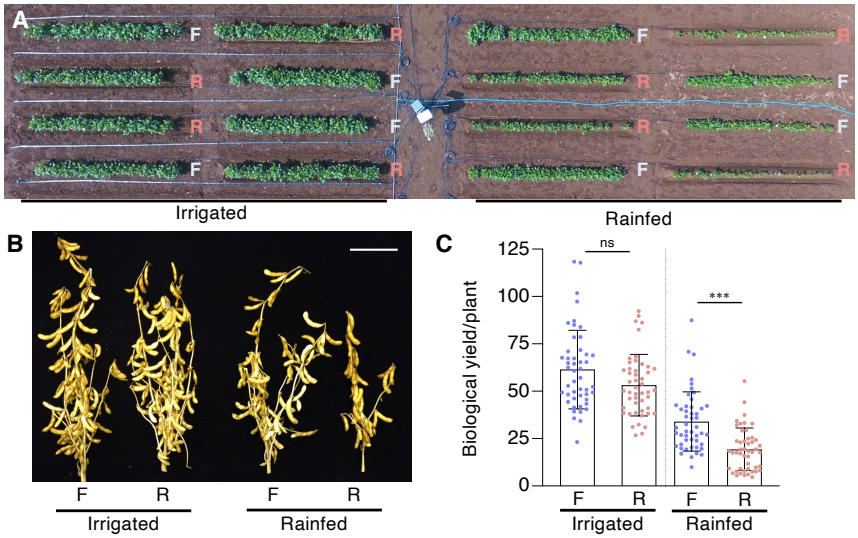

Fig. 2. Irrigation compensates for the reduced growth of plants on ridges. (**A**) Aerial view of 7-week-old soybean plants in the 2018 test. F and R denote flats and ridges, respectively. Left half, irrigated area. Right half, rainfed area. (**B**) Representative view of soybean plants from the flats and ridges with and without irrigation. Scale bar, 10 cm. (**C**) Biological yield (total dry weight of seed, stem, and pod shells) per plant grown on the flats and ridges (n = 48). $^{***}P < 0.001$, Brown-Forsythe and Welch ANOVA tests with Dunnett's T3 multiple comparisons test; ns, no significant difference. Error bars denote SD.

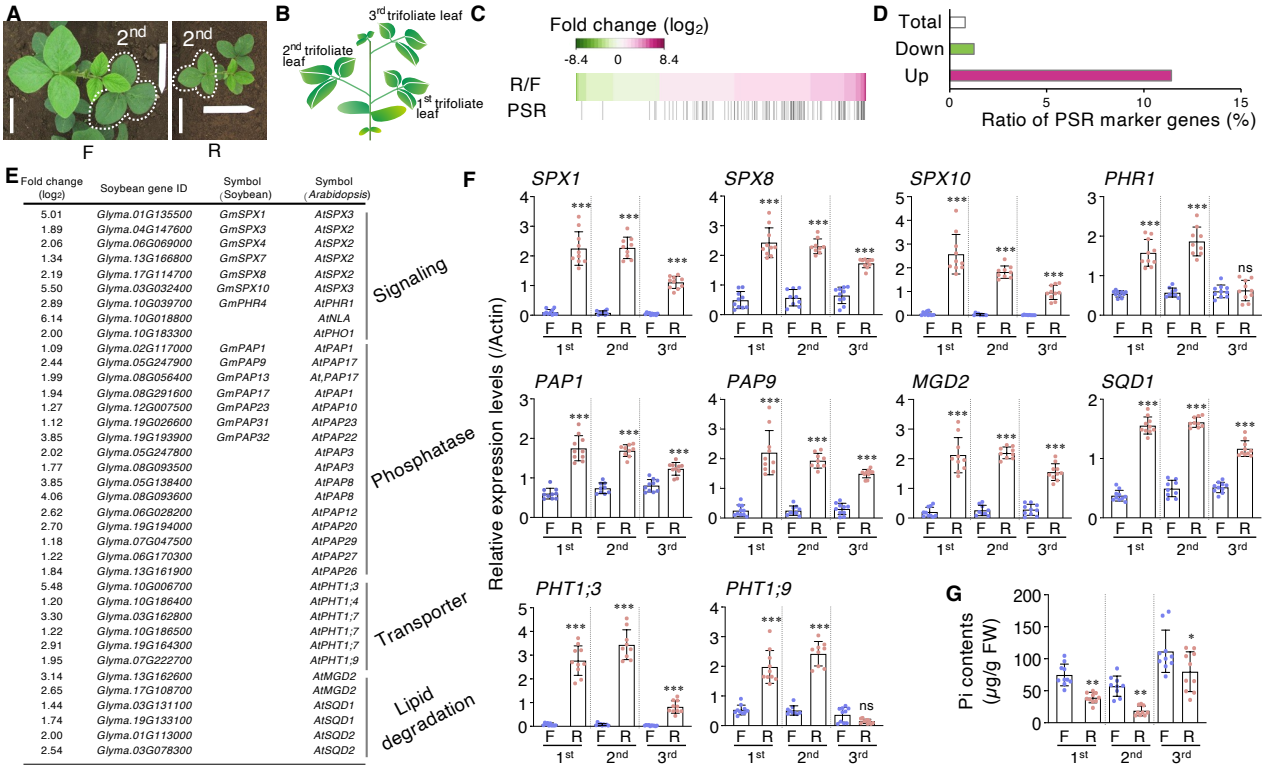

Fig. 3. Mild drought induces PSR in field-grown soybean plants. (**A**) Positions of the second trifoliate leaves (dotted enclosure) used for RNA-seq analysis, in 30-day-old soybean plants grown on flats and ridges in 2015. Scale bars, 10 cm. (**B**) Schematic representation of a soybean plant. (**C**) Heat map of $\log_2$ fold change in expression of 990 up-regulated and 400 down-regulated genes ($|\log_2(FC)| \geq 1$, FPKM value > 0, $q < 0.05$) under mild drought conditions induced by ridges. Lower row indicates PSR genes. (**D**) Ratio of PSR marker genes to the total number of up- and down- regulated genes, respectively. (**E**) A list of representative up-regulated PSR marker genes under mild drought conditions. (**F**) PSR gene expression with quantitative RT-PCR in first to third trifoliate leaves of 29-day-old plants grown on ridges and flats in 2015 ($n = 9$ in second trifoliate leaves; $n = 10$ in first and third trifoliate leaves). F and R denote flats and ridges, respectively. (**G**) Pi contents of first to third trifoliate leaves in soybean plants grown on ridges and flats in the same samples as described in (F). $^{*}P < 0.05$, $^{**}P < 0.01$, and $^{***}P < 0.001$ [one-way analysis of variance (ANOVA) with Tukey's test], in ridged versus flat plots for each leaf position; ns, no significant difference. Error bars denote SD.

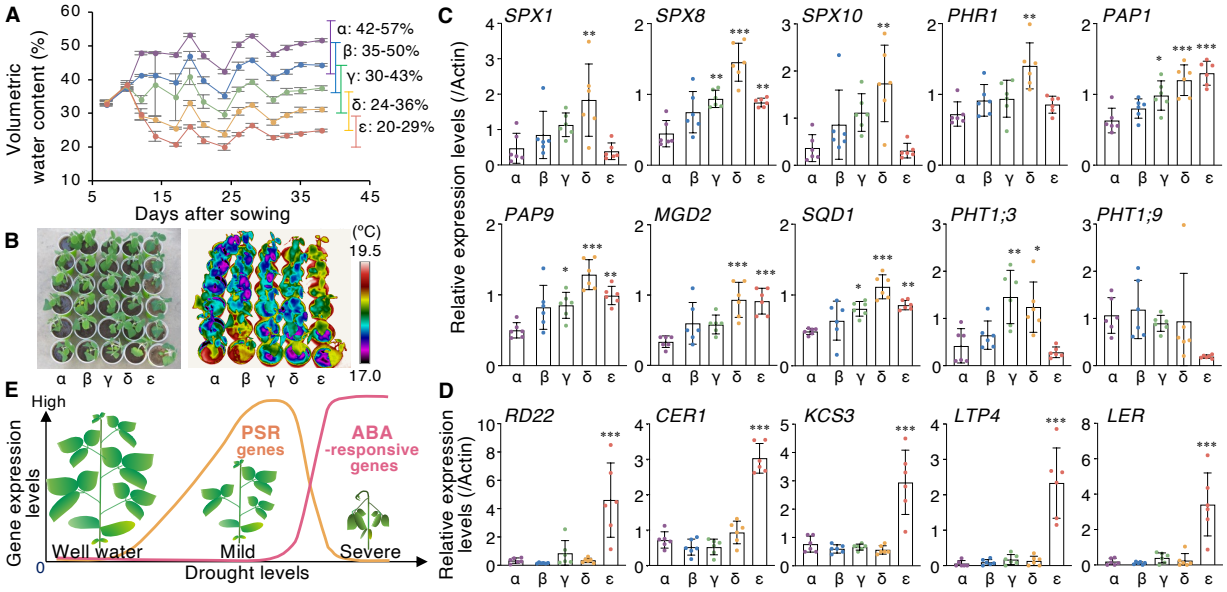

Fig. 4. Mild and severe water deficit induce the PSR and ABA response, respectively. (**A**) Time-course analysis of VWCs in potted soybean plants with five different moisture contents (n = 6). The range of variation in VWCs during the period from day 7 after sowing (when plants were transplanted into pots) to day 38 (when sampling was done) is shown on the right. From 10 days after sowing, we started the drought stress treatments. (**B**) Thermogram and the corresponding digital image of 26-day-old soybean plants in the pots. (**C** and **D**) Relative expression of PSR (C) and ABA responsive (D) genes in the V1 leaves of the 38-day-old plants shown in (B), as determined by quantitative RT-PCR (n = 6). $^{*}P < 0.05$, $^{**}P < 0.01$, and $^{***}P < 0.001$ [one-way analysis of variance (ANOVA) with Tukey's test], in β–ε versus α. Error bars denote SD. (**E**) Proposed model of the plant's response in terms of gene expression to increasing levels of water deficit stress.